Journal of Organometallic Chemistry 693 (2008) 2767–2774

Contents lists available at ScienceDirect

Journal of Organometallic Chemistry

journal homepage: www.elsevier.com/locate/jorganchem

Synthesis, structures, electrochemistry and electrocatalysis of two novel copper(II) complexes constructed with aromatic polycarboxylates and dipyrido[3,2-d:2′,3′-f]quinoxaline

Xiu-Li Wang *, Hong-Yan Lin, Guo-Cheng Liu, Hai-Yan Zhao, Bao-Kuan Chen

Faculty of Chemistry and Chemical Engineering, Bohai University, Jinzhou 121000, PR China

ARTICLE INFO

Article history:
Received 11 April 2008
Received in revised form 17 May 2008
Accepted 23 May 2008
Available online 28 May 2008

Keywords:
Hydrothermal synthesis
Copper complexes
Crystal structures
Electrocatalysis

ABSTRACT

Two novel coordination polymers $[Cu_3(1,3\text{-}BDC)_4(Dpq)_2]$ (**1**) and $[Cu_2(BTC)(OH)(Dpq)_2]\cdot H_2O$ (**2**), have been hydrothermally synthesized by self-assembly of aromatic polycarboxylate ligands 1,3-H_2BDC (1,3-H_2BDC = 1,3-benzenedicarboxylate) or H_3BTC (H_3BTC = 1,3,5-benzenetricarboxylate), chelating ligand Dpq (Dpq = dipyrido[3,2-d:2′,3′-f]quinoxaline), and copper chloride. X-ray diffraction analysis reveals that each trinuclear Cu^{II} cluster is bridged by two coordination modes of 1,3-BDC ligands to form one-dimensional (1-D) chain structure in complex **1**. Complex **2** possesses a two-dimensional (2-D) layer network composed of dinuclear $[Cu_2(OH)(Dpq)_2]$ unit and bridging ligand BTC. The adjacent chains for **1** or the adjacent layers for **2** are further linked by π–π stacking interactions to form the three-dimensional (3-D) supramolecular frameworks. Moreover, the electrochemical properties of the two copper(II) complexes bulk-modified carbon paste electrodes (Cu-CPEs: **1**-CPE and **2**-CPE) have been studied, and the results indicate that both Cu-CPEs give one-electron quasi-reversible redox waves in potential range of 600 to −400 mV due to the metal copper ion Cu(II)/Cu(I). The Cu-CPEs have good electrocatalytic activities toward the reduction of nitrite and bromate in 0.1 M pH 2 phosphates buffer solution, and have remarkable long term stability and especially good surface renewability by simple mechanical polishing in the event of surface fouling, which is important for practical application.

1. Introduction

The design and construction of infinite high-dimensional metal–organic frameworks (MOFs) has become the object of much current study, owing to their intriguing framework topologies as well as their potential applications in catalysis, nonlinear optics (NLO), molecular adsorption and magnetic materials [1,2]. In particular, exploring rigid polycarboxylates ligands and suitable metal salts to construct novel architectures is of higher interest [3]. Among them, aromatic polycarboxylates are often employed in a design strategy to construct coordination compounds with special topologies due to the predictability of the resulting networks [4,5]. Such as, 1,3,5-benzenetricarboxylate (H_3BTC), 1,3-benzenedicarboxylate (1,3-H_2BDC), 1,2,4,5-benzenetetracarboxylate (1,2,4,5-H_4btec), 1,4-benzenedicarboxylate (1,4-H_2BDC), are one kind of the successful multifunctional ligands because of their structural rigidity, chemical stability, and appropriate connectivity [6–8]. A variety of MOFs with diversified topologies and interesting properties have been prepared based on these aromatic polycarboxylates [2c,5,9].

Recently, aromatic polycarboxylic acid, 2,2′-bipyridyl-like chelating ligands, and their analogues have been extensively utilized to bridge the metal centers, leading to interesting MOF structures and properties [7c,7d,10]. The aromatic chelate ligands are also important in maintaining the one dimensionality and may provide potential supramolecular recognition sites for π–π aromatic stacking interactions to form high-dimensional supramolecular networks [11]. Dipyrido[3,2-d:2′,3′-f]quinoxaline (Dpq) is one of the typical 2,2′-bipyridyl-like chelating ligands, however, the studies based on Dpq have been less reported [12]. As an extension of our study of metal/Dpq/carboxylates hybrid systems, we have been focusing on using hydrothermal reactions to prepare new high-dimensional metal–organic frameworks [13].

On the other hand, great efforts have been directed towards the study of Cu^{II} complexes of chelating ligands incorporating pyridine, thioether, imidazole and imine donors, which not only stem from their fascinating structures but also from their potential applications as new materials [14]. Meanwhile, several groups have investigated the electrochemistry and electrocatalysis of copper complexes with various different ligands. Our group have studied the electrocatalytic reduction of NO_2^- by copper(II) complexes with Dpq $[Cu_2(Dpq)_2(Ac)_2(H_2O)_2](ClO_4)_2\cdot H_2O$, and the results showed that NO_2^- is reduced to N_2O through one-electron

* Corresponding author. Tel.: +86 416 3400158.
E-mail address: wangxiuli@bhu.edu.cn (X.-L. Wang).

0022-328X/$ - see front matter © 2008 Elsevier B.V. All rights reserved.
doi:10.1016/j.jorganchem.2008.05.031

reduction of Cu(II)/Cu(I) [15]. In this paper, we report two novel copper compounds: $[Cu_3(1,3\text{-BDC})_4(Dpq)_2]$ (**1**) and $[Cu_2(BTC)(OH)(Dpq)_2]\cdot H_2O$ (**2**), with bpy-like chelating ligand Dpq and BDC/or BTC as mixed ligands (Chart 1a). In addition, the electrochemistry properties for the two compounds bulk-modified carbon paste electrodes (CPE) have been examined.

2. Results and discussion

2.1. Description of the structure

The multi-carboxylate groups on the aromatic ring may be completely or partially deprotonated, so 1,3-BDC and BTC ligands have a great ability to construct coordination architectures with metal ions, adopting several different coordination fashions, ranging from unidentate to chelating to bridging, sometimes in more than one way in the same architecture [16]. In our work, 1,3-BDC adopted two different coordination modes in complex **1** (Chart 1b), and BTC adopted only one coordination modes in complex **2** (Chart 1c), as shown in Chart 1. In the two complexes, ligand Dpq takes a chelating coordination mode while the other two nitrogen atoms did not coordinated to the metal ions.

$[Cu_3(1,3\text{-BDC})_4(Dpq)_2]$ (**1**): X-ray study reveals that complex **1** is a 1-D coordination polymer chains constructed from trinuclear copper clusters and 1,3-BDC linkers. As shown in Fig. 1, the fundamental building unit of the crystal structure for **1** is composed of two kinds of crystallographical independent Cu^{II} centers [Cu(1), Cu(2)]. The Cu(2) center is penta-coordinated by three oxygen atoms belonging to three different carboxylate groups from three separated 1,3-BDC ligands [the distances: Cu(2)–O(1), 1.941(3); Cu(2)–O(3), 1.938(3); Cu(2)–O(6), 2.283(3) Å], and two nitrogen atoms from a chelating ligand Dpq with the bond distances 2.008(4) [Cu(2)–N(1)] and 2.012(3) Å [Cu(2)–N(2)], showing a distorted tetragonal pyramid geometry. The other Cu^{II} center [Cu(1)] is four coordinated by four oxygen atoms [O(2), O(2A), O(5), O(5A)] of four different carboxylate groups from four separated 1,3-BDC ligands with distances 1.917(2) and 1.9414(19) Å, respectively. All the above distances are within the normal range [17].

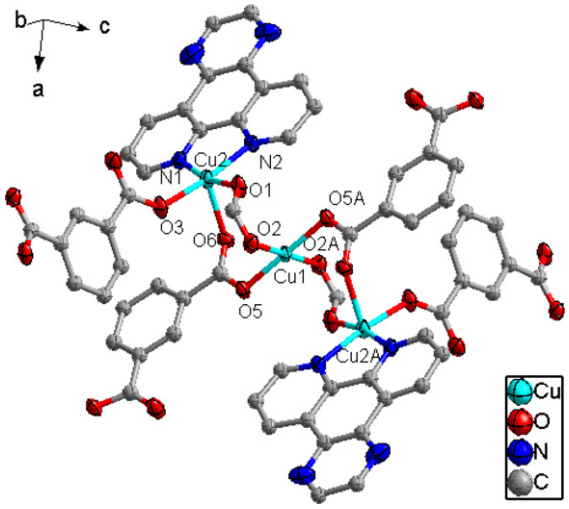

Fig. 1. ORTEP diagram showing the coordination environment for Cu atoms in **1** (at 50% probability level).

Three adjacent metal ions [Cu(2), Cu(1), Cu(2A)] are connected by 1,3-BDC ligands showing two different coordination modes (unidentate-bidentate and bidentate, see Chart 1b) to construct a trinuclear cluster $[Cu_3(Dpq)_2(O_2C-)_6]$, in which the non-bonding distances of Cu···Cu are 3.721(5) Å [Cu(1)···Cu(2)], and 7.443(6) Å [Cu(2)···Cu(2A)], respectively. The coordination modes of 1,3-BDC in complex **1** are different from in reference 12d. 1,3-BDC only exhibits one bis(unidentate) coordination mode as bridging ligand to link two Cu^{II} ions for the compound $[Cu(1,3\text{-BDC})(Dpq)(H_2O)]\cdot C_4H_9NO\cdot H_2O$ in reference 12d. The structural differences of two compounds illustrate that the influence of coordination modes of bridging ligand 1,3-BDC in the self-assembly of polymeric coordination architectures.

Adjacent trinuclear clusters are connected by bidentate-monodentate bridging ligands 1,3-BDC to form 1-D infinite chain, as shown in Fig. 2. Moreover, the 1-D chains are extended to 2-D

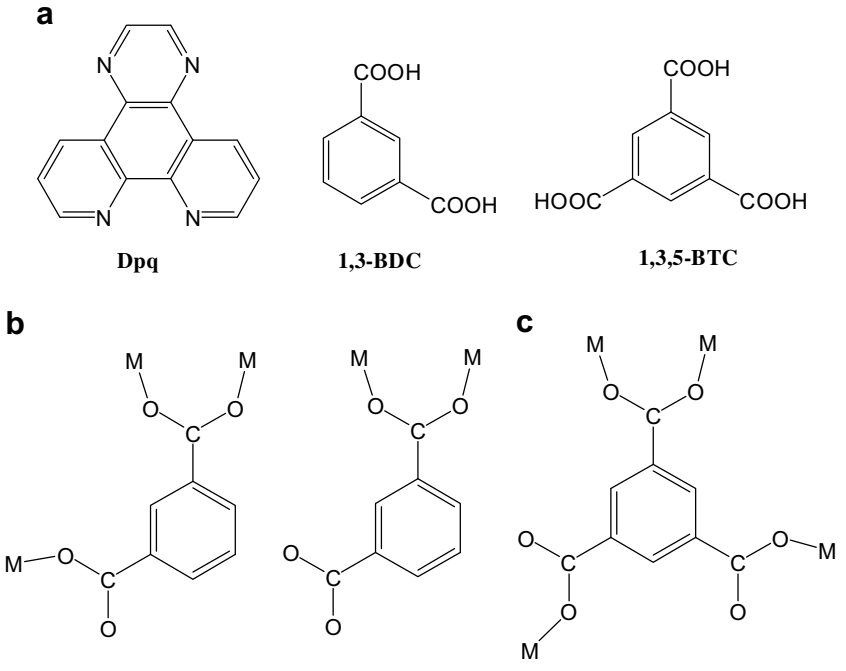

Chart 1. Ligands (a), coordination modes of 1,3-BDC for **1** (b) and BTC for **2** (c).

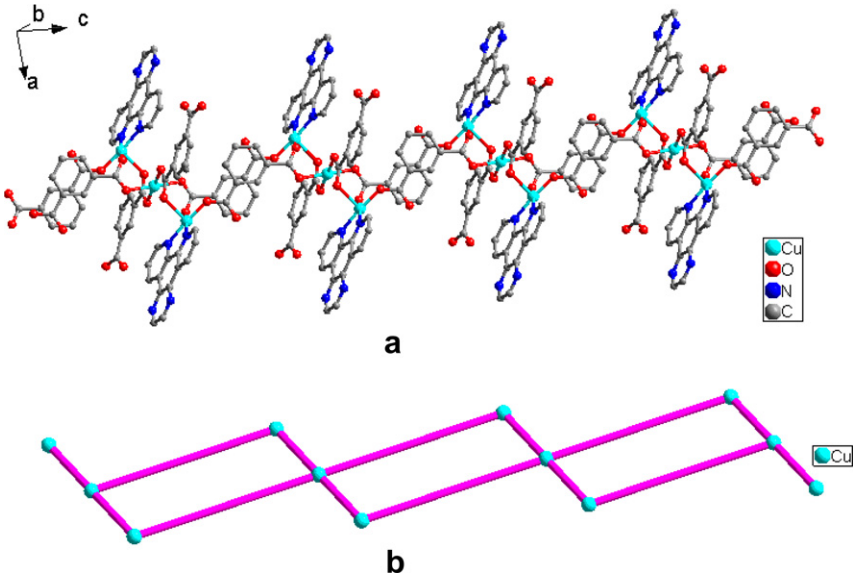

Fig. 2. (a) 1-D polymeric chain of **1**; (b) the schematic of 1-D polymeric ribbon in **1**.

network by π–π stacking interaction among the aromatic rings of Dpq ligands with face-to-face distance ca. 3.57 Å (see Fig. 3), or π–π stacking interaction between the aromatic rings of Dpq ligands and the aromatic rings of 1,3-BDC ligands with face-to-face distance ca. 3.52 Å (Fig. S1, supporting information). Additionally, the 2-D networks are ultimately packed into a 3-D supramolecular structure through the two kinds of π–π stacking interaction along *c*-axis, see Fig. 4. In complex **1**, there exists a weak hydrogen bonding between carboxylate oxygen atoms and the Dpq carbon atoms with O···C distances of 3.058(8) Å [C(7)···O(6)], 3.381(6) Å [C(18)···O(7)], the hydrogen bonding angles being 122° and 147°, respectively. The weak hydrogen bonding interactions consolidate the 3-D supramolecular framework of **1**.

$[Cu_2(BTC)(OH)(Dpq)_2]\cdot H_2O$ (**2**): X-ray study reveals that complex **2** is a 3-D supramolecular network based on 2-D polymer layer composed of dinuclear copper building unit $[Cu_2(OH)(Dpq)_2]$ and bridging ligand BTC. The coordination environment of Cu(II) is shown in Fig. 5. In the dinuclear structure of **2**, the Cu(II) center is coordinated by two nitrogen atoms from one Dpq ligand with Cu–N distances ranging from 2.011(4) to 2.069(4) Å, two carboxylate oxygen atoms from two BTC ligands with Cu–O distances 1.965(3)–2.220(3) Å, and a hydroxyl oxygen atom [Cu(1)–O(1) = 1.913(3) and Cu(2)–O(1) = 1.894(3) Å], showing a penta-coordination environment. The $Cu–O_{Hydroxo}$ bond lengths are within normal range [17], and the Cu···Cu separation distance (3.431 Å) is similar to other dinuclear Cu^{II}-bis(μ-hydroxo) complexes [17d]. In compound **2**, BTC adopted only one coordination modes, but three carboxylate groups of the BTC link three Cu^{II} ions with two different coordination modes (see Chart 1c): unidentate mode and bidentate mode. One carboxylate group links two Cu^{II} ions [Cu(1) and Cu(2)] of one dinuclear $[Cu_2(OH)(Dpq)_2]$ unit through bidentate bridging mode, the other two carboxylate groups links two Cu^{II} ions [Cu(1) and Cu(2)] from two different dinuclear $[Cu_2(OH)(Dpq)_2]$ units in unidentate mode. Each dinuclear unit $[Cu_2(OH)(Dpq)_2]$ is linked by three BTC bridges to form a 2-D layer network, as shown in Fig. 6 (and Fig. S2, supporting information).

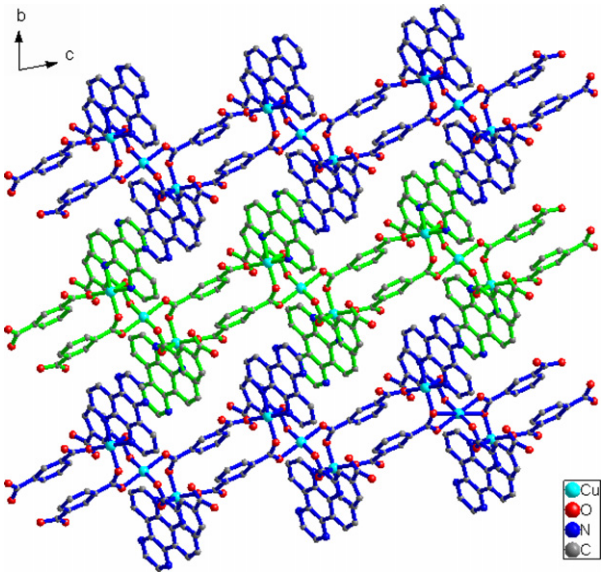

Fig. 3. 2-D supramolecular network of **1** formed by π–π stacking interaction among the aromatic rings of Dpq along *a*-axis (H atoms are omitted for clarity).

For perspicuous representation, the dinuclear units are represented as nodes and BTC linkers are represented by triangular units. The framework can be described as a distorted mesh network, in which each dinuclear unit connects to three BTC linkers and each BTC linker connects to three dinuclear units (Fig. 7). Ligand Dpq, as a heteroatoms cycle ligand is adpt to form the potential π–π stacking interaction to enhance the stability of the polymers [11]. Notably, there exist weak π–π interactions between Dpq ligands in neighboring layers for **2** (ca. 3.68 Å, see Fig. 8) [11d], resulting in a 3-D supramolecular network. Moreover, the stability of 3-D supramolecular network in **2** was strengthened by the coexistence of two kinds of hydrogen bonding interactions [O···O hydrogen bonding: O(1W)···O(2) = 2.774(8) Å, O(1W)···O(6) = 2.899(10) Å; and C···O hydrogen bonding: C(12)···O(1W) = 3.135(10) Å; C(18)···O(6) = 3.198(8) Å].

2.2. Infrared spectra

The main features in the IR spectra of **1**–**2** mainly concern the carboxylate groups and the ligand Dpq (Figs. S3 and S4, supporting information). The IR spectra display the typical stretching bands of carboxylate groups between 1300 and 1640 cm^{-1}, a very strong

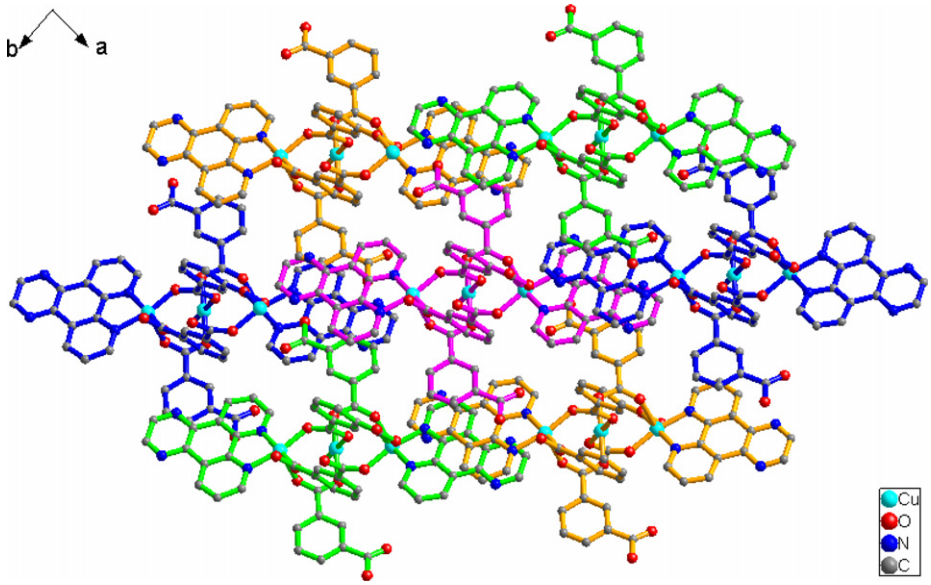

Fig. 4. 3-D supramolecular network of **1** formed by π–π stacking interaction between the aromatic rings of Dpq, π–π stacking interaction between the aromatic rings of Dpq and 1,3-BDC along *c*-axis (H atoms are omitted for clarity).

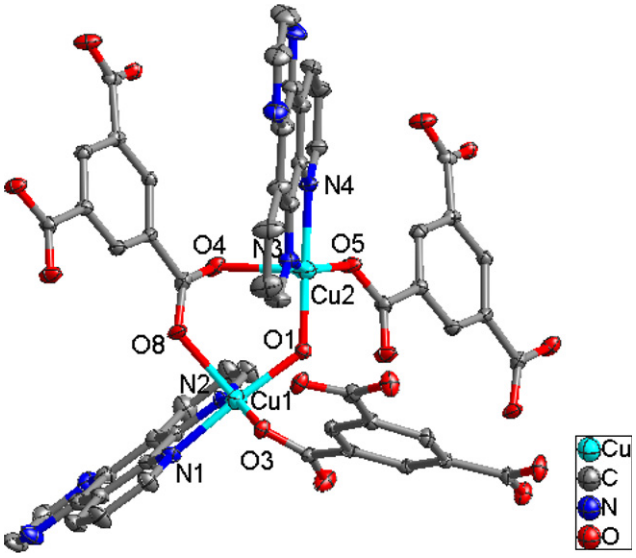

Fig. 5. ORTEP drawing (at 30% probability level) of the coordination environment of Cu(II) ions in **2** (for clarity, the H atoms are not shown).

band appears at around 1620 cm^{-1} due to the asymmetric stretching (ν_{as}) of the carboxylate group; the symmetrical stretching (ν_s) band of this group appears at 1482–1629 and 1366–1480 cm^{-1}, respectively. The bands at about 1560, 1480, 1080, and 705 cm^{-1} may be attributed to the ν_{C-N} stretching of the pyridyl ring or pyrazinyl ring. No strong absorption peaks around 1700 cm^{-1} for –COOH are observed, indicating that carboxyl groups of organic moieties in **1**–**2** are completely deprotonated [10c,18]. Weak absorptions observed at 2920–3085 cm^{-1} for **1**–**2** can be attributed to the ν_{C-H} of the pyridyl group. The strong broad bond at around 3500 cm^{-1} is assigned to the vibrations of hydroxyl groups.

2.3. Thermal stability analysis

To examine the thermal stability of title compounds, thermal gravimetric (TG) analyses were carried out for **1** and **2** in the temperature range of 30–630 °C (Figs. S5 and S6, supporting information). The TG curve of complex **1** exhibits only one obvious weight loss step, the decomposition of organic ligands Dpq and 1,3-BDC occurring between 260 and 370 °C. It gives a total weight loss of 82.08%, which agrees with the calculated value of 81.70%. The remaining weight (17.92%) indicates that the final product should be CuO (calc. 18.30%). While for complex **2**, two weight loss steps were observed. The continuous weight loss step from 170 to 280 °C is attributed to the loss of the lattice water molecule. The weight loss is about 2.53%, in correspondence with the calculated value of 2.16%. The sharp weight loss was observed in the range 330–470 °C, corresponding to the decomposition of organic ligands (78.75%, calculated value of 78.64%). The remaining weight (18.82%) corresponds to the percentage (19.20%) of Cu and O components in CuO, indicating this is the final product.

2.4. Electrochemical behavior of the Cu-CPEs

The electrochemical studies of the two copper complexes modified CPE (Cu-CPEs) were carried out in 0.1 M phosphates buffer aqueous solution (pH 2). Fig. 9 shows the cyclic voltammograms at a bare CPE and the modified CPEs. It can be seen from Fig. 9 that in the potential range 600 to −400 mV, there is no redox peak at the bare CPE. While at the modified Cu-CPEs, a redox couple attributed to the redox of Cu(II)/Cu(I) was observed [14c,14d,19]. The mean peak potentials $E_{1/2} = (E_{pa} + E_{pc})/2$ were −31 mV and −44 mV for **1**-CPE and **2**-CPE, respectively. In fact, there was a large reduction wave due to $Cu(II) + e^- \rightarrow Cu(I)$ while the oxidation wave was quite small. This was most possibly due to the instability of the reduced form of complex which can undergo a fast chemical oxidation in an aqueous solution of pH 2.0 [20]. The cyclic voltammograms exhibited one anodic and cathodic peak corresponding to redox system Cu(II)/Cu(I), which showed a quasi-reversible behavior in an aqueous medium [21].

Scan rates effect on the electrochemical behavior of the Cu-CPEs was investigated in the potential range of +600 to −400 mV in 0.1 M pH 2 phosphates buffer aqueous solution as shown in Fig. 10. When the scan rate was varied from 20 to 500 mV s^{-1}, the peak potentials change gradually: the cathodic peak potentials shifted to negative direction and the corresponding anodic peak potentials shifted to positive direction with increasing scan rate.

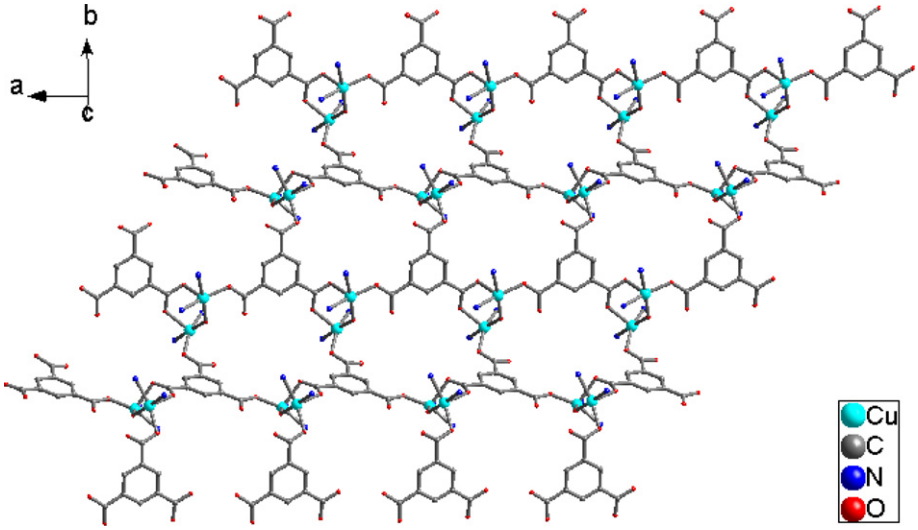

Fig. 6. View of the 2-D layer framework of **2**. (H atoms and part of the aromatic rings are omitted for clarity).

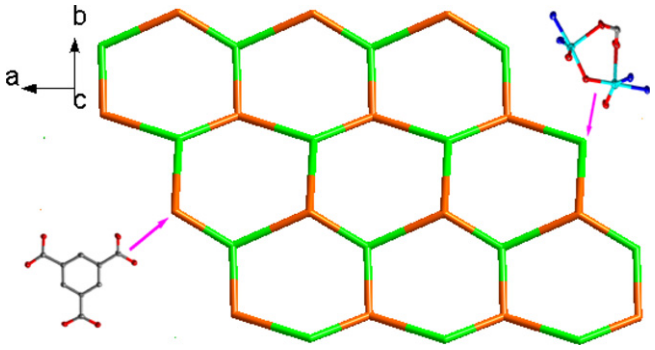

Fig. 7. Schematic of 2-D mesh network formed in **2**.

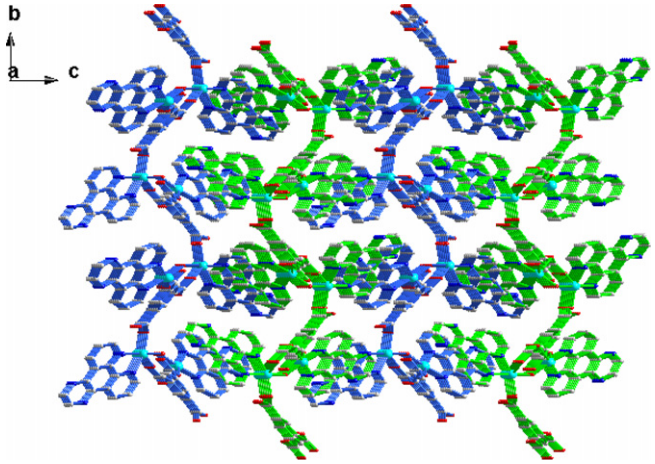

Fig. 8. 3-D network structure of **2** formed by π–π stacking interaction between the aromatic rings of Dpq (H atoms are omitted for clarity).

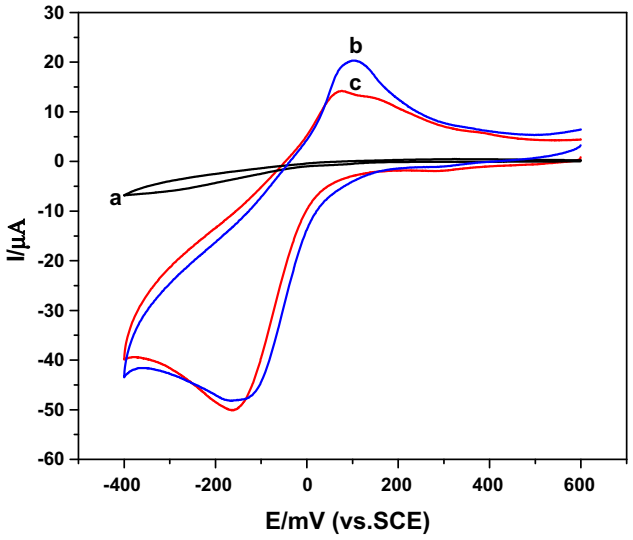

Fig. 9. Cyclic voltammograms of (a) the bare CPE, (b) **1**-CPE and (c) **2**-CPE in 0.1 M pH 2 phosphates buffer solution in the potential range of 600 to −400 mV. Scan rate: 100 mV s^{-1}.

The plots of peak currents versus scan rates were shown in inset of Fig. 10. As shown in inset of Fig. 10a, the anodic and the cathodic currents were proportional to the scan rate, suggesting that the redox process for **1**-CPE was surface-confined process. While for **2**-CPE at scan rates lower than 120 mV s^{-1}, the peak currents were proportional to the scan rates, which indicated the redox process of **2**-CPE was surface-controlled; however, at scan rates higher than 120 mV s^{-1}, the peak currents were proportional to the square root of the scan rate, which indicated the redox process of **2**-CPE was diffusion-controlled (inset in Fig. 10b). The different results of the Cu-CPEs may be attributed to the different structures of copper complexes.

2.5. Electrocatalytic activity of the Cu-CPEs

2.5.1. Electrocatalytic reduction towards bromate

Bromate is a disinfectant by-product contaminant found in drinking water, and is formed during the ozonation of source water containing bromide. The overpotential for BrO_3^- reduction is high and therefore an efficient electrocatalyst would be beneficial [22]. The reduction of BrO_3^- is totally irreversible at a glassy carbon electrode in acidic aqueous solution and does not take place prior to the evolution of hydrogen [23]. However, the reduction of BrO_3^- can readily be catalyzed by Cu-CPEs in pH 2 phosphate buffer solution. Fig. 11 and Fig. S7 (supporting information) show the comparative cyclic voltammograms for the electroreduction of

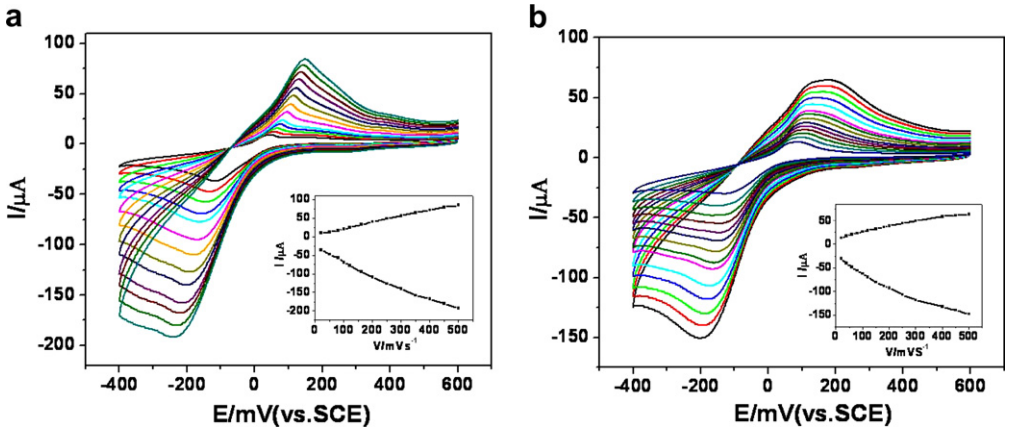

Fig. 10. Cyclic voltammograms of Cu-CPEs in pH 2 phosphate buffer solution at different scan rates (from inner to outer) 20, 50, 80, 100, 120, 150, 200, 250, 300, 350, 400, 450, and 500 mV s^{-1}, (a) for **1**-CPE, (b) for **2**-CPE. The inset shows the plots of the anodic and the cathodic peak currents vs. scan rates.

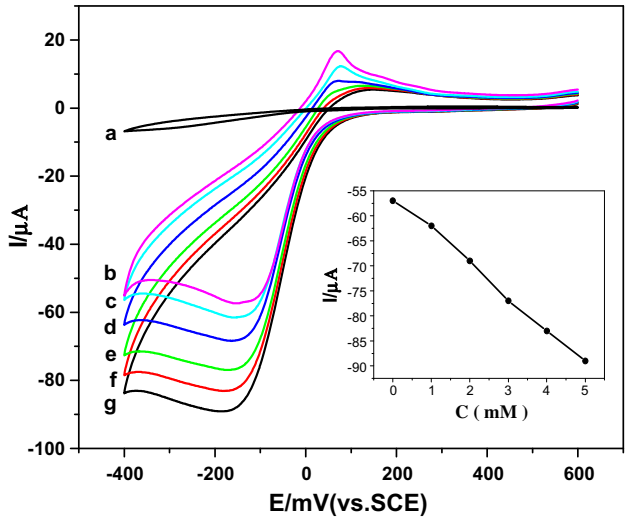

Fig. 11. Cyclic voltammograms of a bare CPE containing 2 mM $KBrO_3$ (a) and **1**-CPE in pH 2 phosphate buffer solution containing BrO_3^- concentrations of 0.0 (b), 1 (c), 2 (d), 3 (e), 4 (f), 5 (g) mM. Scan rate: 80 mV s^{-1}. Inset: the variation of cathodic peak currents vs. bromate concentrations.

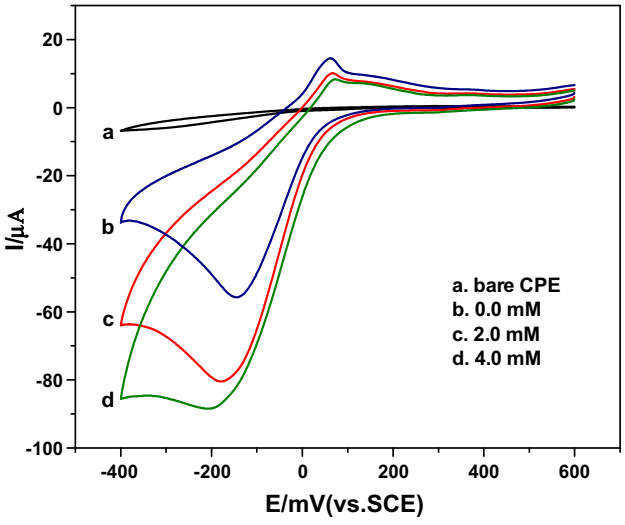

Fig. 12. Cyclic voltammograms of a bare CPE in phosphate buffer solution with pH of 2 containing 2 mM $NaNO_2$(a) and **1**-CPE in phosphate buffer solution containing NO_2^- concentrations of 0.0 (b), 2 (c), 4 (d) mM. Scan rate: 100 mV s^{-1}.

bromate at the surface of bare CPE and Cu-CPEs in the absence and presence of bromate in pH 2 buffer solution. Upon the addition bromate there was a dramatic enhancement of the cathodic peak current and the anodic peak current decreased, which indicated a strong catalytic effect. The insets of Fig. 11 and Fig. S7 show that catalytic currents were linear with BrO_3^- concentration up to 5 or 10 mM. The electrochemical behaviors and the electrocatalytic activities of Cu-CPEs are similar to that of our report in Ref. [15].

2.5.2. Electrocatalytic reduction towards nitrite

The electrocatalytic reduction of nitrite in pH 2 phosphate buffer solution was investigated at the title complexes modified CPEs, as shown in Fig. 12 (and Fig. S8, supporting information). It is well known that direct electroreduction of nitrite ion requires a large overpotential at most electrode surfaces and no obvious response is observed at a bare CPE. Our results indicate that Cu-CPEs have good electrocatalytic activity toward the reduction of nitrite. With the addition of nitrite, the reduction peak currents increase markedly while the corresponding oxidation peak currents decrease markedly. Based on the results, the electrochemical catalytic pathway is probably the reduction of NO_2^- to form NO and then further reduction to N_2O in the acidic aqueous solution [14e]. We have also note that high scan rate (100 mV s^{-1}) has been used to register the electrocatalytic reduction of nitrite for **1**-CPE and obtained noticeable catalytic currents, which indicates the reduction of nitrite at **1**-CPE are fast.

2.6. Repeatability of surface-renewal and long-term stability

Compared with other modified film electrodes, the three-dimensional bulk-modified Cu-CPEs show high stability. The electrodes can be renewed by squeezing a little carbon paste out glass tube and a fresh surface is exposed whenever needed. This is especially useful for electrocatalytic study since the catalytic activity is known to decrease when the electrode is fouled. When the potential range was maintained at 600 to −400 mV, it was stable over 500 cycles at a scan rate of 100 mV s^{-1} and the current response remained almost unchanged. When the Cu-CPEs were stored at room temperature for at least 4 months, the current response decreased only 4%. Moreover, experimental results show that the two Cu-CPEs give superior stability compared with the Cu-CPE in Ref. [15]. The better stability of the Cu-CPEs could be ascribed primarily to the insolubility of the copper complexes synthesized through hydrothermal method.

2.7. Conclusions

Two novel copper complexes, $[Cu_3(1,3\text{-}BDC)_4(Dpq)_2]$ (**1**) and $[Cu_2(BTC)(OH)(Dpq)_2]\cdot H_2O$ (**2**), were synthesized under the hydrothermal condition and structurally characterized by X-ray diffraction analyses. Two complexes exhibit 1-D chain and 2-D layer structures, respectively. And the adjacent chains in **1** and the adjacent layers in **2** are further linked by π–π stacking interactions to form 3-D supramolecular framework. The complexes **1** and **2** were employed to fabricate the bulk-modified carbon paste electrodes (Cu-CPEs: **1**-CPE and **2**-CPE) due to their insolubility. The Cu-CPEs show good electrocatalytic activities toward the reduction of bromate and nitrite. These preliminary results in this work represent potential applications in the field of electrocatalysis.

3. Experimental

3.1. Materials and methods

All reagents employed were commercially available and used as received without further purification. Dpq were synthesized by the methods of the literature [24]. FT-IR spectra (KBr pellets) were taken on a Magna FT-IR 560 Spectrometer and the elemental analyses (C, H, and N) were carried out on a Perkin–Elmer 240C elemental analyzer. Thermogravimetric analysis was carried out with a Pyris Diamond TG-DTA instrument. The electrochemical experiments were carried out using a CHI 440 Electrochemical Quartz Crystal Microbalance. A conventional three-electrode cell was used at room temperature. The modified electrode was used as working electrode. A SCE and a platinum wire were used as reference and auxiliary electrodes, respectively.

3.2. Preparation of the compounds

Synthesis of $[Cu_3(1,3\text{-}BDC)_4(Dpq)_2]$ (**1**): Compound **1** was prepared by simple hydrothermal reaction of $CuCl_2\cdot 2H_2O$ (0.034 g, 0.2 mmol), 1,3-H_2BDC (0.0332 g, 0.2 mmol), Dpq (0.023 g, 0.1 mmol), H_2O (12 mL) and NaOH (0.016, 0.4 mmol), the mixture was stirred for 30 min in air, then transferred and sealed in a 25 mL Teflon reactor, which was heated at 160 °C for 6 days leads to the formation of blue block crystals **1** (29% yield based on Cu). Anal. Calc. for $C_{60}H_{32}N_8O_{16}Cu_3$: C, 54.90; H, 2.46; N, 8.54%. Found: C, 54.78; H, 2.62; N, 8.42%. IR (KBr, cm^{-1}): 3415s, 3087m, 3011w, 2919w, 2355m, 2332m, 1624s, 1570s, 1479m, 1433s, 1410m, 1380s, 1326s, 1258m, 1210w, 1128w, 1075m, 999m, 816m, 740s, 709s, 664m, 595w, 564w, 518m.

Synthesis of $[Cu_2(BTC)(OH)(Dpq)_2]\cdot H_2O$ (**2**): A mixture of $CuCl_2\cdot 2H_2O$ (0.034 g, 0.2 mmol), H_3BTC (0.025 g, 0.12 mmol), Dpq (0.023 g, 0.1 mmol), H_2O (12 mL) and NaOH (0.015 g, 0.37 mmol) was stirred for 30 min in air, then transferred and sealed in a 25 mL Teflon reactor, which was heated at 160 °C for 6 days leads to the formation of yellow block crystals, and washed by water, ethanol, dried in air. Yield: ~25% (based on Cu). Anal. Calc. for $C_{37}H_{22}N_8O_8Cu_2$: C, 53.30; H, 2.66; N, 13.45. Found: C, 53.18; H, 2.85; N, 13.56%. IR (KBr, cm^{-1}): 3430s, 3082w, 2927w, 2355m, 2332m, 1621s, 1552s, 1482m, 1435w, 1413m, 1350s, 1227w, 1127m, 1065s, 1034w, 949w, 810m, 763s, 725s, 702m, 663w, 624w, 532w.

3.3. Preparation of modified CPEs

The modified CPEs were fabricated as follows: 0.5 g graphite powder and 0.035 g compounds **1** (or **2**) were mixed and ground together by agate mortar and pestle for approximately 20 min to achieve an even, dry mixture; to the mixture 0.20 mL paraffin oil was added and stirred with a glass rod; then the homogenized mixture was used to pack 3 mm inner diameter glass tubes to a length of 0.8 cm. The electrical contact was established with the copper stick, and the surface of the modified CPEs was wiped with weighing paper. The same procedure was used for preparation of bare CPE without copper complex.

Table 1
Crystal data and structure refinement for complexes **1**–**2**

	1	**2**
Formula	$C_{60}H_{32}Cu_3N_8O_{16}$	$C_{37}H_{22}Cu_2N_8O_8$
Formula weight	1311.59	833.73
Crystal system	Triclinic	Orthorhombic
Space group	$P\bar{1}$	$P2_12_12_1$
a (Å)	10.344(4)	10.039(5)
b (Å)	11.236(4)	15.379(8)
c (Å)	11.627(2)	21.480(11)
α (°)	79.103(13)	90.00
β (°)	85.05(2)	90.00
γ (°)	83.280(19)	90.00
V (Å^3)	1315.0(7)	3317(3)
Z	1	4
D_{Calc} (g cm^{-3})	1.656	1.670
μ (mm^{-1})	1.287	1.353
$F(000)$	663.0	1688.0
θ_{max} (°)	26.00	27.00
Total data	6078	19374
Unique data	5169	7223
Flack parameters		0.014(15)
R_{int}	0.0295	0.0507
R_1[a] $[I > 2\sigma(I)]$	0.0488	0.0464
wR_2[b] (all data)	0.1583	0.1144
GOF	1.030	1.043
$\Delta\rho_{max}$ (e Å^{-3})	1.572	1.204
$\Delta\rho_{min}$ (e Å^{-3})	−0.364	−0.476

[a] $R_1 = \sum||F_o| - |F_c||/\sum|F_o|$.
[b] $wR_2 = \sum[w(F_o^2 - F_c^2)^2]/\sum[w(F_o^2)^2]^{1/2}$.

3.4. X-ray crystallographic study

Crystallographic data for two complexes was collected at 293(2) K on a Bruker Smart 1000 CCD diffractometer with Mo Kα (λ = 0.71073 Å) by ω-scan mode. The structure was solved by direct methods using the SHELXS program of the SHELXTL package and refined by full-matrix least-squares methods with SHELXL [25]. Metal atoms in the complex were located from the *E*-maps, and all non-hydrogen atoms were refined anisotropically. For **1** and **2**, hydrogen atoms of the hydroxyl groups could not be located. The hydrogen atoms of the ligand were generated theoretically onto the specific atoms and refined isotropically with fixed thermal factors. A summary of crystal data and structure refinements for the two compounds are provided in Table 1. Selected bond lengths and angles are listed in Tables S1 and S2. The related hydrogen bonding geometries are given in Tables S3 and S4.

Acknowledgements

The supports of Natural Science Foundation of Liaoning Province (No. 20061073) and Education Committee Foundation of Liaoning Province (No. 2006031) are gratefully acknowledged.

Appendix A. Supplementary material

CCDC 678435 and 669532 contain the supplementary crystallographic data for compounds **1** and **2**. These data can be obtained free of charge from The Cambridge Crystallographic Data Centre via www.ccdc.cam.ac.uk/data_request/cif. Supplementary data associated with this article can be found, in the online version, at doi:10.1016/j.jorganchem.2008.05.031.

References

[1] (a) G.F. Swiegers, T.J. Malefetse, Chem. Rev. 100 (2000) 3483;
(b) B. Moulton, M.J. Zaworotko, Chem. Rev. 101 (2001) 1629;
(c) O.M. Yaghi, M. OKeeffe, N.W. Ockwig, H.K. Chae, M. Eddaoudi, J. Kim, Nature 423 (2003) 705;
(d) X.H. Bu, M.L. Tong, H.C. Chang, S. Kitagawa, S.R. Batten, Angew. Chem., Int. Ed. 43 (2004) 192.

[2] (a) C. Qin, X.L. Wang, E.B. Wang, Z.M. Su, Inorg. Chem. 44 (2005) 7122;
(b) B. Kesanli, Y. Cui, M.R. Smith, E.W. Bittner, B.C. Bockrath, W.B. Lin, Angew. Chem., Int. Ed. 44 (2005) 72;
(c) X.L. Wang, C. Qin, E.B. Wang, Z.M. Su, Chem. Eur. J. 12 (2006) 2680.

[3] (a) M.C. Hong, Y.J. Zhao, W.P. Su, R. Cao, M. Fujita, Z.Y. Zhou, A.S.C. Chan, Angew. Chem., Int. Ed. 39 (2000) 2468;
(b) B.L. Chen, M. Eddaoudi, S.T. Hyde, M. O'Keeffe, O.M. Yaghi, Science 291 (2001) 1021;
(c) C.Y. Su, Y.P. Cai, C.L. Chen, M.D. Smith, W. Kaim, H.C. Loye, J. Am. Chem. Soc. 125 (2003) 8595;
(d) W. Zhao, Y. Song, T.A. Okamura, J. Fan, W.Y. Sun, N. Ueyama, Inorg. Chem. 44 (2005) 3330.

[4] (a) R. Sun, Y.Z. Li, J.F. Bai, Y. Pan, Cryst. Growth Des. 7 (2007) 890;
(b) S.N. Wang, H. Xing, Y.Z. Li, J. Bai, Y. Pan, M. Scheer, X.Z. You, Eur. J. Inorg. Chem. 2006 (2006) 3041;
(c) S. Wang, J.F. Bai, H. Xing, Y.Z. Li, Y. Song, Y. Pan, M.F. Scheer, X.Z. You, Cryst. Growth Des. 7 (2007) 747.

[5] (a) Q.G. Zhai, C.Z. Lu, X.Y. Wu, S.R. Batten, Cryst. Growth Des. 7 (2007) 2332;
(b) Y.Q. Lan, X.L. Wang, S.L. Li, Z.M. Su, K.Z. Shao, E.B. Wang, Chem. Commun. (2007) 4863;
(c) X.L. Wang, C. Qin, E.B. Wang, Z.M. Su, L. Xu, S.R. Batten, Chem. Commun. (2005) 4789.

[6] (a) W. Chen, J.Y. Wang, C. Chen, Q. Yue, H.M. Yuan, J.S. Chen, S.N. Wang, Inorg. Chem. 42 (2003) 944;
(b) X.M. Chen, G.F. Liu, Chem. Eur. J. 8 (2002) 4844;
(c) B.H. Ye, M.L. Tong, X.M. Chen, Coord. Chem. Rev. 249 (2005) 545;
(d) Y.B. Go, X.Q. Wang, E.V. Anokhina, A.J. Jacobson, Inorg. Chem. 43 (2004) 5360.

[7] (a) L.Y. Zhang, G.F. Liu, S.L. Zheng, B.H. Ye, X.M. Zhang, X.M. Chen, Eur. J. Inorg. Chem. 2003 (2003) 2965;
(b) Y.G. Li, N. Hao, E.B. Wang, Y. Lu, C.W. Hu, L. Xu, Eur. J. Inorg. Chem. 2003 (2003) 2567;
(c) C.B. Li, W. Fang, G.G. Gao, B. Liu, Acta Crystallogr., Sect. E 62 (2006) 1312;
(d) Q.W. Wang, Q.L. Meng, Z.X. Yu, X.H. Zhao, Acta Crystallogr., Sect. E 62 (2006) 3009.

[8] (a) C.A. Williams, A.J. Blake, P. Hubberstey, M. Schröder, Chem. Commun. (2005) 5435;
(b) B.H. Ye, B.B. Ding, Y.Q. Weng, X.M. Chen, Cryst. Growth Des. 5 (2005) 801;
(c) D.F. Sun, R. Cao, Y.C. Liang, Q. Shi, M.C. Hong, J. Chem. Soc., Dalton Trans. (2002) 1847.

[9] (a) L.H. Xie, S.X. Liu, B. Gao, C.D. Zhang, C.Y. Sun, D.H. Li, Z.M. Su, Chem. Commun. (2005) 2402;
(b) Q.R. Fang, G.S. Zhu, M. Xue, Z.P. Wang, J.Y. Sun, S.L. Qiu, Cryst. Growth Des. 8 (2008) 319;
(c) F. Luo, Y.X. Che, J.M. Zheng, Eur. J. Inorg. Chem. 2007 (2007) 3906;
(d) J. Zhang, Y.B. Chen, S.M. Chen, Z.J. Li, J.K. Cheng, Y.G. Yao, Inorg. Chem. 45 (2006) 3161.

[10] (a) S.M.F. Lo, S.S.Y. Chui, L.Y. Shek, Z.Y. Lin, X.X. Zhang, G.H. Wen, I.D. Williams, J. Am. Chem. Soc. 122 (2000) 6293;
(b) K. Barthelet, J. Marrot, D. Riou, G. Férey, Angew. Chem., Int. Ed. 41 (2002) 281;
(c) X.J. Gu, D.F. Xue, Cryst. Growth Des. 6 (2006) 2551;
(d) G. Marinescu, M. Andruh, M. Julve, F. Llusar, S. Uriel, J. Vaissermann, Cryst. Growth Des. 5 (2005) 261.

[11] (a) X.M. Chen, G.F. Liu, Chem. Eur. J. 8 (2002) 4811;
(b) M.L. Tong, H.J. Chen, X.M. Chen, Inorg. Chem. 39 (2000) 2235;
(c) X.M. Zhang, M.L. Tong, S.H. Feng, X.M. Chen, J. Chem. Soc., Dalton Trans. (2001) 2069;
(d) Gary S. Nichol, William Clegg, Cryst. Growth Des. 6 (2006) 451.

[12] (a) G.B. Che, C.B. Liu, B. Liu, Q.W. Wang, Z.L. Xu, CrystEngComm 10 (2008) 184;
(b) Z.B. Han, X.N. Cheng, X.M. Chen, Cryst. Growth Des. 5 (2005) 695;
(c) G.B. Che, C.B. Liu, Acta Crystallogr., Sect. E 62 (2006) 1728;
(d) W.Z. Zhang, Acta Crystallogr., Sect. E 63 (2007) 1692.

[13] (a) X.L. Wang, Y.F. Bi, G.C. Liu, H.Y. Lin, T.L. Hu, X.H. Bu, CrystEngComm (2008) 349;
(b) X.L. Wang, Y.F. Bi, H.Y. Lin, G.C. Liu, Cryst. Growth Des. 7 (2007) 1086;
(c) X.L. Wang, H.Y. Lin, T.L. Hu, J.L. Tian, X.H. Bu, J. Mol. Struct. 798 (2006) 34.

[14] (a) R. Balamurugan, M. Palaniandavar, M.A. Halcrow, Polyhedron 25 (2006) 1077;
(b) E.H. Kim, D.I. Kim, H.S. Lee, J.C. Byun, J.H. Choi, Y.C. Park, Polyhedron 26 (2007) 85;
(c) G.G. Gao, L. Xu, W.J. Wang, W.J. An, Y.F. Qiu, Z.Q. Wang, E.B. Wang, J. Phys. Chem. B 109 (2005) 8948;
(d) A. Salimi, V. Alizadeh, H. Hadadzadeh, Electroanalysis 16 (2004) 1984;
(e) S.M. Chen, J. Electroanal. Chem. 457 (1998) 23.

[15] X.L. Wang, H.Y. Zhao, H.Y. Lin, G.C. Liu, J.N. Fang, B.K. Chen, Electroanalysis 20 (2008) 1055.

[16] (a) J.C. Dai, X.T. Wu, Z.Y. Fu, C.P. Cui, S.M. Hu, W.X. Du, L.M. Wu, H.H. Zhang, R.Q. Sun, Inorg. Chem. 41 (2002) 1391;
(b) X.L. Wang, Y.F. Bi, H.Y. Lin, G.C. Liu, B.K. Chen, J. Organomet. Chem. 692 (2007) 4353.

[17] (a) K.L.V. Mann, J.C. Jeffery, J.A. Mecleverty, P. Thornton, M.D. Ward, J. Chem. Soc., Dalton Trans. (1998) 89;
(b) S. Hikichi, M. Yoshizawa, Y. Sasajura, M. Ajita, Y. Moroja, J. Am. Chem. Soc. (1998) 10567;
(c) C.M. Liu, D.Q. Zhang, D.B. Zhu, Cryst. Growth Des. 3 (2003) 363;
(d) G.S. Patricia, G.T. Javier, D.G. Virginia, G.G. Rubén, L.P. José, Inorg. Chem. Commun. 8 (2005) 259.

[18] L.J. Bellamy, The Infrared Spectra of Complex Molecules, Wiley, New York, 1958.

[19] B.K. Santra, P.A.N. Reddy, G. Neelakanta, S. Mahadevan, M. Nethajia, A.R. Chakravartya, J. Inorg. Biochem. 89 (2002) 191.

[20] N. Fay, E. Dempsey, T. Mccormac, J. Electroanal. Chem. 574 (2005) 359.

[21] J.N. Younathan, K.S. Wood, T.J. Meyer, Inorg. Chem. 31 (1992) 3280.

[22] G.L.L. Gonzalez, H. Kahlert, F. Scholz, Electrochim. Acta 52 (2007) 1968.

[23] X.L. Wang, E.B. Wang, Y. Lan, Electroanalysis 14 (2002) 1116.

[24] J.G. Collins, A.D. Sleeman, J.R. Aldrich-Wright, I. Greguric, T.W. Hambley, Inorg. Chem. 37 (1998) 3133.

[25] (a) G.M. Sheldrick, SHELXS-97, Program for Crystal Structure Solution, Göttingen University, Germany, 1997;
(b) G.M. Sheldrick, SHELXL-97, Program for Crystal Structure Refinement, Göttingen University, Germany, 1997.